Supported by tetfund TERTIARY EDUCATION TRUST FUND

Fluid Flow past a Vertical Porous Plate in Unsteady MHD Heat and Mass Transfer in the Presence of Variable Suction, Reynolds Number, and Chemical Reaction.

O. L. Ahmed[1], A. Jimoh[2], A. M. Ayinde[3*], G. Ajileye[4]

[1]Department of Mathematical Sciences, Base University, Abuja, Nigeria.
[2]Nigerian Communication Satellite Limited, Airport Road, Abuja, Nigeria.
[3*]Department of Mathematics, Modibbo Adama University, Yola, Nigeria.
[4]Department of Mathematics, Federal University, Wukari, Nigeria.
*Corresponding author email: abdullahim@mautech.edu.ng

Received: March 20, 2022 **Accepted:** June 18, 2022

Abstract: The impacts of magnetohydrodynamic (MHD) heat and mass transfer fluid flow via a vertical porous plate with varying suction, Reynolds number, and chemical reaction are investigated in this work. With appropriate boundary conditions, the governing boundary-layer equations are fomulated in the (x^* , y^* , t^*) coordinate system. For non-scattering medium, the Rosseland diffusion approximation is used to analyze the radioactive heat flux. The Crank-Nicolson method was used to solve the model's governing equations, which were simplified, non-dimensionalyzed, and solved. The effects of magnetic field, dissipation function, Prandtl number, radiation-conduction parameter, thermal Grashof number, species Grashof number, Schimdt number, Reynolds number, and chemical reaction are examined on the dimensionless velocity, temperature, and species function distributions. The variation of local skin friction, Nusselt number, and Sherwood number are also computed to examine their impacts on the flow. The results show that while Reynolds number (Re) increases with velocity and temperature, the concentration remains constant.

Keywords: Reynolds Number, Mass Transfer, Variable suction, MHD, Chemical Reaction and Heat Generation.

Introduction

The study of MHD heat and mass transfer fluid flow through a vertical porous plate with variable suction, Reynolds number, and chemical reaction effects has piqued the interest of a large number of researchers due to its extensive applications in various disciplines of science and engineering. These applications include the industrial processes like drying, cooling of nuclear reactors chemical deposition on surfaces, magneto hydrodynamic (MHD) power generators, solar physics, astrophysical studies and polymer technology. Heat and mass transfer problem in a porous medium has important applications in geothermal reservoir, geothermal extraction and heat exchangers. The Reynolds number (Re) is a dimensionless number in fluid mechanics which gives a measure of the ratio of inertial to viscous forces and therefore measures the relative importance of these two types of forces for given flow conditions. The incompressible Navier-Stokes equations can be stated in non-dimensional form, with the Reynolds number as the only parameter, in addition to measuring the ratio of inertial to viscous forces in a flow (ignoring body forces).

This modification simplifies the work and often formed the basis for the validity of wind tunnel testing. Also, effects of magnetic field on viscous incompressible fluid of electrically conducting is of importance in many applications such as extrusion of plastics in the manufacture of Rayon and Nylon, purification of crude oil, textile industries. Rushikumai *et al.*(2012) studied MHD free convection flow between two parallel porous walls with varying temperature. In their analysis, similarity variable was used to reduce the partial differential equations into ordinary differential equations. Their reduced equations were solved using shooting method. Subhakar *et al.* (2012) studied Soret and Dufour effects on MHD free convection heat and mass transfer flow over a stretching vertical plate with suction and heat source/sink. When the thermal condition of a fluid is at high temperature, the influence of thermal radiation is also high. Many engineering problems occur at higher temperature. Despite the role of thermal radiation on fluid flow, it is unfortunate that many researchers in the field of fluid dynamics neglect its effect in their investigations. Idowu *et al.* (2013) applied the analytical method to solve the heat and mass transfer of magnetohydrodynamics (MHD) and dissipative fluid flow pass in a moving vertical porous plate with variable suction.

Attention has been focused in recent years by various scientists and engineers in the study of problem involving the phenomena of heat and mass transfer with radiation effect. This interest is due to the fact that the effect of radiation on convection is quite important in the context of many practical applications such as in cooling and heating of channels, nuclear power plant, fire research, electrical power generation, gas turbines and nuclear waste disposal. Uwanta & Usman (2014) has mentioned the convective heat and mass transfer flow over a vertical plate with nth-order chemical reaction in an exceedingly porous medium. Uwanta & Usman (2015) solved the problem of finite difference solutions of magneto-hydrodynamic free convective flow with constant suction and variable thermal conductivity in an exceedingly Darcy-Forchheimer porous medium. Given the effect of magnetohydrodynamics free convection flow with thermal radiation and chemical reaction effects in the presence of variable suction, Usman *et al.* (2016), Thermal radiation and Soret-associated Dufour effects on the unsteady heat and mass transfer flow of a chemically reacting fluid pass a semi-infinite vertical plate with viscous dissipation were examined by Alao *et al.* (2016). In their research, they used the spectral relaxation method to numerically to solve the transformed dimensionless equations by introducing non-dimensional quantities to their governing partial differential equations. Their result shows that increasing the thermal radiation parameter decreases the temperature distribution with a cooled plate. Kala *et al.* (2017) discovered Diffusion-thermo and thermo-diffusion effects on MHD fluid flow over Non-linearly stretching sheet through a Non- Darcy porous medium. They used similarity transformations to reduce the governing equations to ordinary differential equations in their research. Bvp4c MATLAB is then used to solve the transformed equations. They discovered that as the Dufour number rises, the Sherwood number rises as well. Dimensionless time, thermal Grashof number, species Grashof number, Reynolds number, Eckert number, Prandtl number, Schmidt number, and chemical reaction are shown to be governed by the following thermophysical parameters. Impact of these parameter on velocity, temperature, and concentration profiles Also given and explored are local shared stress and local sherwood numbers are presented and discussed. As a result, this research looks into the effects of MHD heat and mass transfer fluid flow past a vertical porous plate with variable suction, Reynolds number, and chemical reaction, as inspired by several applications of the effects of these

parameters on MHD free convection flow, such as the design of temperature control devices in the satellite industry and filtration processes in the chemical industry.

Problem Formulation

In the presence of a transverse magnetic field with viscous dissipation, we study an unsteady one-dimensional laminar natural convection flow of a viscous, incompressible, electrically conducting, and radiating fluid past an impulsively initiated semi-infinite vertical plate. It's supposed that the fluid is grey, absorbing-emitting but non-scattering. The y^* -axis is chosen perpendicular to the plate at the leading edge, whereas the x^* -axis is chosen vertically upwards along the plate. The origin of the x^* -axis is assumed to lie at the plate's leading edge. The gravitational acceleration g occurs in a downward direction. The plate and the fluid are assumed to be at the same ambient temperature T_∞^* and species concentration C_∞^* at time t^* =0. When $t^* > 0$, the plate temperature and species concentration are maintained to be T_w^* (greater than T_∞^*) and C_w^* (greater than C_∞^*), respectively. In the binary mixture, the influence of viscous dissipation is considered, and it is believed to be very small in comparison to the other chemical species present. In the flow direction, a uniformly transverse magnetic field is applied. The interaction of the induced magnetic field with the flow is also believed to be negligible in comparison to the interaction of the applied magnetic field with the flow. Except for the body force elements in the momentum equation, which are approximated by Boussinesq relations, the fluid properties are assumed to be constant. Thermal radiation is assumed to exist in the y^* direction as a unidirectional flux, i.e., q_r (transverse to the vertical surface). Following Modest (1993), the Rosseland diffusion flux is utilized and defined as follows:

$$q_r = -\frac{4\sigma}{3k^1}\frac{\partial T^{*4}}{\partial y^*} \tag{1}$$

k^1 is the mean absorption coefficient, while σ is the Stefan-Boltzmann constant. It should be emphasized that the current research is confined to optically thick fluids due to the use of the Rosseland approximation. The boundary layer equations for mass, momentum, energy, and species conservation in a (x^*, y^*) coordinate system may be demonstrated to have the following form using the Boussinesq approximation:

Mass Conservation

$$\frac{\partial u^*}{\partial y^*} = 0 \tag{2}$$

Momentum Conservation

$$\frac{\partial u^*}{\partial t^*} + v^*\frac{\partial u^*}{\partial y^*} = \nu\frac{\partial^2 u^*}{\partial y^{*2}} + g\beta\left(T^* - T_\infty^*\right) + {}^2$$

$$g\beta^*\left(C^* - C_\infty^*\right) - \frac{\sigma}{\rho}B_O^2 u^* - \frac{\nu}{k}u^* - \frac{b}{\rho k}u^* \tag{3}$$

Energy Equation

$$\frac{\partial T^*}{\partial t^*} + v^*\frac{\partial T^*}{\partial y^*} = \alpha\frac{\partial^2 T^*}{\partial y^{*2}} + \frac{\nu}{C_p}\left[\frac{\partial u^*}{\partial y^*}\right]^2 -$$

$$\frac{1}{\rho C_p}\frac{\partial q_r}{\partial y^*} + \frac{\nu}{C_p}\left(\frac{\partial u^*}{\partial y^*}\right)^2 + \frac{\alpha_T}{\rho C_p}(T^* - T_\infty^*) \tag{4}$$

Species Conservation

$$\frac{\partial C^*}{\partial t^*} + v^*\frac{\partial C^*}{\partial y^*} = D\left[\frac{\partial^2 C^*}{\partial y^{*2}}\right] \tag{5}$$

The corresponding initial and boundary conditions are prescribed as follows:

$$t^* \le 0, U^* = 0, T^* = T^*{}_\infty, C^* = C^*{}_\infty,$$
$$t^* > 0, U^* = U^*{}_0, T_w^* = T^*{}_\infty, C_w^* = C^*{}_\infty, \quad at\ y^* = 0,$$
$$U^* \to 0, T^* \to T^*{}_\infty\ C^* \to C^*{}_\infty \quad as\ y^* \to \infty. \tag{6}$$

x^* and y^* are coordinates, u^* and v^* are velocity components in the x^* and y^* directions, t^* is dimensionless time, σ is the Stefan-Boltzmann constant, g is gravitational acceleration, k^1 is the mean absorption coefficient of thermal expansion, β is the mass transfer coefficient of expansion, ν is the grey fluid's kinematic viscosity, T^* is the temperature of the fluid in the boundary layer, C^* is the species concentration, k is the permeability(hydraulic conductivity of the porous medium with dimensions m^2), α is the thermal diffusivity, D is the species diffusivity, The condition at the wall denoted by $()_w$, and the condition in the free stream is denoted by $()_\infty$ (outside the boundary layer). If the temperature differences within the flow are sufficiently small, we can express the quartic temperature function as a linear function of temperature, as Raptis and Perdikis (1999) did. The Taylor series for T^{*4}, discarding higher order terms can be shown as

$$T^{*4} \approx 4T^{*3}{}_\infty T^* - 3T^{*4}{}_\infty \tag{7}$$

Substituting the above equation (7) into equation (4) then into the energy equation gives

$$\frac{\partial T^*}{\partial t^*} + v^*\frac{\partial T^*}{\partial y^*} = \alpha\frac{\partial^2 T^*}{\partial y^{*2}} + \frac{\nu}{C_p}\left[\frac{\partial u^*}{\partial y^*}\right]^2 + \frac{16\sigma T_\infty^{*3}}{3k^1\rho C_p}\frac{\partial^2 T^*}{\partial y^{*2}} \tag{8}$$

Equations (2), (3), (5) and (8) with boundary conditions (6) constitutes a two-point boundary value problem which is fairly challenging to solve. We therefore use non-dimensionalise model to facilitate a numerical solution by the Crank Nicolson's method.

Transformation of the Model

$$X=\frac{x^*u_0^*}{\nu},Y=\frac{y^*u_0^*}{\nu},U=\frac{u^*}{u_0^*},V=\frac{v^*}{u_0^*},E_c=\frac{u_0^*}{C_p\left(T_w^*-T_\infty^*\right)}$$

$$t=\frac{t^*u_0^{*2}}{\nu},\theta=\frac{T^*-T_\infty^*}{T_w^*-T_\infty^*},C=\frac{C^*-C_\infty^*}{C_w^*-C_\infty^*},Re=\frac{u_0^*L}{\nu}$$

$$Pr=\frac{\nu}{\alpha},Sc=\frac{\nu}{D},Da=\frac{k}{L^2},N=\frac{k^1k}{4\sigma T_\infty^{*3}}$$

$$Gr=\frac{g\beta\nu\left(T_w^*-T_\infty^*\right)}{u_0^{*3}},Gm=\frac{g\beta^*\nu\left(C_w^*-C_\infty^*\right)}{u_0^{*3}},M=\frac{\sigma B_0^2\nu}{\rho U_0^{*2}}$$

$$S=\frac{k\left(T_w-T_\infty\right)}{T_r} \quad (9)$$

T is the dimensionless temperature function, C is the dimensionless concentration function, and N is the dimensionless numeric value. X and Y are dimensionless coordinates, U and V are dimensionless velocities, t is dimensionless time, T is the

$$\frac{\partial T}{\partial t}-\tau\frac{\partial T}{\partial Y}=\frac{1}{Pr}\left[1+\frac{4}{3N}\right]\frac{\partial^2T}{\partial Y^2}+Ec\left[\frac{\partial U}{\partial Y}\right]^2+ST \quad (12)$$

$$\frac{\partial C}{\partial t}-\tau\frac{\partial C}{\partial Y}=\frac{1}{Sc}\frac{\partial^2C}{\partial Y^2}. \quad (13)$$

Employing the non-dimensional quantities stated in equation (9), the Nusselt, local skin friction, and Sherwood number in dimensionless form becomes;

$$\tau=\frac{\tau_x}{\rho u_0^{*2}}=-\frac{\partial U}{\partial Y} \quad (15)$$

$$Nu_x=-X\frac{\partial T}{\partial Y} \quad (16)$$

Dimensionless temperature function, C is the dimensionless concentration function, and N is the dimensionless numeric value. Pr is the Prandtl number, Sc is the Schimdt number, Re is the Reynold number, Gr is the thermal Grashof number, and Gm is the species Grashof number, M is the magnetic field parameter, and Ec is the Eckert number at the conduction-radiation heat transfer parameter. When these transformations are introduced into equations (2), (3), (5), and (8), they are reduced to the dimensionless equations:

$$\frac{\partial U}{\partial Y}=0 \quad (10)$$

$$\frac{\partial U}{\partial t}-\tau\frac{\partial U}{\partial Y}=GrT+GmC+\frac{\partial^2U}{\partial Y^2}-MU-\frac{U}{Re^2Da}-\frac{FsU^2}{DaRe} \quad (11)$$

The corresponding initial and boundary conditions take the form

$$t\le 0,U=0,T=0,C=0,$$

$$t>0,U=1,T=1,C=1,\quad at\ Y=0,$$

$$U\to 0,T\to 0\ C\to 0\quad as\ Y\to\infty.$$

$$Sh_x=-X\frac{\partial C}{\partial Y} \quad (17)$$

The derivatives involved in equations (15) to (18) are evaluated using a five-point approximation formula.

Numerical Solution

To solve these unsteady coupled non-linear partial differential equations (10 to 13) under the boundary conditions (14), we employ an implicit finite difference scheme of the Crank-Nicolsons type. This method has been extensively developed in recent years and remain one of the best reliable method for solving partial differential equation. The partial differential equations are converted to difference equation. The Crank-Nicolson method has been used in several heat transfer, radiation and convection flow problems. Ransom and Fulton (1985), discussed a modified, optimized version of the method for general thermal engineering problems. Prasad *et al.* (2006) used Crank-Nicolson scheme to analyse the transient convective heat and mass transfer with thermal radiation effects along a vertical impulsively started plane. The method has been found to work efficiently for parabolic type of partial differential equations. We define the co-ordinate, (y,t) of the mesh points of the solution domain by $y=j\Delta y$ and $t=k\Delta t$ where j,k are positive integers and we denote the values of U at these mesh points by $U(j\Delta y,k\Delta t)=U_j^k$. The finite difference equation corresponding to these equations are given as follows:

$$\frac{\left[U_j^{k+1}-U_j^k\right]}{\Delta t}-\tau\frac{\left[U_{j+1}^{k+1}-U_{j-1}^{k+1}+U_{j+1}^k-U_{j-1}^k\right]}{4\Delta Y}=Gr\frac{\left[T_j^{k+1}+T_j^k\right]}{2}+Gm\frac{\left[C_j^{k+1}+C_j^k\right]}{2}+\frac{\left[U_{j-1}^{k+1}-2U_j^{k+1}+U_{j+1}^{k+1}+U_{j-1}^k-2U_j^k+U_{j+1}^k\right]}{2(\Delta Y)^2}-\frac{1}{DaRe^2}\frac{\left[U_j^{k+1}+U_j^k\right]}{2}-M\frac{\left[U_j^{k+1}+U_j^k\right]}{2} \quad (18)$$

$$\frac{\left[T_j^{k+1}-T_j^k\right]}{\Delta t}-\tau\frac{\left[T_{j+1}^{k+1}-T_{j-1}^{k+1}+T_{j+1}^k-T_{j-1}^k\right]}{4\Delta Y}=Ec\left[\frac{[U_{j+1}^k-U_j^k]}{2\Delta Y}\right]^2-(R-S)\frac{\left[T_j^{k+1}+T_j^k\right]}{2}+\frac{\left[T_{i,j-1}^{k+1}-2T_j^{k+1}+T_{j+1}^{k+1}+T_{j-1}^k-2T_j^k+T_{j+1}^k\right]}{2(\Delta Y)^2} \quad (19)$$

$$\frac{\left[C_j^{k+1}-C_j^k\right]}{\Delta t}-\tau\frac{\left[C_{j+1}^{k+1}-C_{j-1}^{k+1}+C_{j+1}^k-C_{j-1}^k\right]}{4\Delta Y}=\frac{1}{Sc}\frac{\left[C_{j-1}^{k+1}-2C_j^{k+1}+C_{j+1}^{k+1}+C_{j-1}^k-2C_{i,j}^k+C_{j+1}^k\right]}{2(\Delta Y)^2} \quad (20)$$

The region of integration is defined as a rectangle with sides $Y_{(max)}$, where $Y_{(max)}$ corresponds to $Y=\infty$, and lies well outside the momentum, thermal, and concentration boundary

layers where considered. Along the $Y-$ direction, and $k-$ along the $t-$ direction, the subscript $j-$ implies. As a result, we divide Y into N grid spacing, respectively. $\Delta Y = 0.05$ and $\Delta t = 0.01$ are the mesh sizes used. C, T, and U values are known at all grid points throughout the computations because of the initial conditions. C, T, and U values at time level $(k+1)$ are computed from known values at time level (k). Hence, for every internal nodal point on a given $j-$ level, the finite difference equation becomes a tridiagonal system of equations, which is solved using the Matlab programming tool, which applies the Thomas Algorithm as detailed in Carnahan et al. (1969).

As a result, for each i at $(k+1)th$ time level, we calculated the values of C and T at each nodal point, and the results were used in U at the $(k+1)th$ time level. The values of C, T, and U are thus known at all grid points at time level $(k+1)$. The process is repeated for various $j-$ levels until the steady-state is attained, which is assumed to have occurred when the absolute difference between the values of U, T and C at two consecutive time steps is less than $10^{(-5)}$ at all grid points. The local truncation error is $0(\Delta t^2 + \Delta Y^2)$ and it tends to zero as $\Delta t, \Delta Y, and \Delta X$ tends to zero, which indicates that the system is compatible. Hence, since the Crank-Nicolson system is always unconditionally stable, hence, the compatibility and stability ensures the convergence.

Results and Discussion

Series of computation has been carried out for the effects of controlling fluid parameters on the velocity, temperature and concentration as well as local skin friction, Nusselt number and sherwood number. The present analysis concerns the case of optically thick boundary layers, where thermal boundary layer is expected to become very thick as the medium is highly absorbing. The Rosseland diffusion model adds a radioactive conductivity to the conventional thermal conductivity. The effect of radiation on temperature profile is decreasing while the effect Reynolds number is increasing along the temperature profile.

The effects of Gr and Gc on the velocity profile against the Y co-ordinate are shown in Figures 1 and 2. The relative impacts of thermal buoyance force on the viscous hydrodynamic force in the boundary layer are indicated by Gr and Gc. Increases in Gr and Gc cause the steady state velocity profiles to rise. The increase gives a rapid rise in the velocity near the wall, followed by a gradual descent to zero. Figure 3 illustrates the Viscous dissipation function K on the dimensionless velocity profile. We observed from this figure, that increase in the dissipation function K, from 0.01 to 0.07 induces a substantial rise in the velocity profile.

Figure 4 also depicts the magnetic parameter M as it increases. As a result, the velocity profile decreases. When a magnetic field is applied to an electrically conducting fluid, it produces a resistive force known as the Lorentz force, which has the propensity to slow down the fluid's velocity and raise its temperature.

It can be seen from Figure 5 and 6 that the velocity of the fluid increases with the increase of fluid parameter Pr while the radiation parameter R decreases as velocity profile increasing. Figures 7, 12, and 13 show the effects of various suction parameter τ values on velocity, temperature, and species concentration profiles. The concentration and temperature rise as the value of the τ parameters rises, whereas the velocity profile. Decreases as the value of the τ parameters increases.

The influence of Prandtl number and radiation parameters on the temperature distribution in a stream-wise direction is shown in Figures 8 and 9. With an increase in R, the temperature profile decreases, whereas the effects of Pr on the temperature profile decrease with an increase in Pr.

The temperature rises with increasing S, as shown in Figure 10. Figure 11 also illustrates that the temperature rises as the Reynolds number of the fluid parameter Re rises.

Figures 11 and 12 show the impact of Schmidt number and chemical Kr reaction on concentration. As the Schmidt number increases, so does the concentration profile. It's worth noting that when the Schmidt number rises, the concentration boundary layer thickens. The concentration buoyancy effect in the fluid concentration increases as a result of this.

In terms of physics, a rise in Sc corresponds to a rise in molecular diffusivity. While the concentration falls as the chemical reaction parameter Kr increases, the concentration boundary layer grows thinner. We found that increasing the Eckert number, Ec, from 100,000 to 400,000 induces a substantial rise in the temperature profile in figure 16.

For various values of the Reynolds number, Schmidtl number, thermal Grashof number, and species Grashof number, the table below displays the numerical values of local skin friction, local Nusselt number, and local Sherwood number with stream-wise distance

X. Local skin friction increases as Gr increases, as shown in the table below.

For varied values of Re, we noticed that as the numerical value of Re increases, the Reynolds number on the local Nusselt number also increases. Also, we noticed for the local Sherwood profiles against Sc with various values that the sherwood numbers increases due to the presence of viscous dissipative.

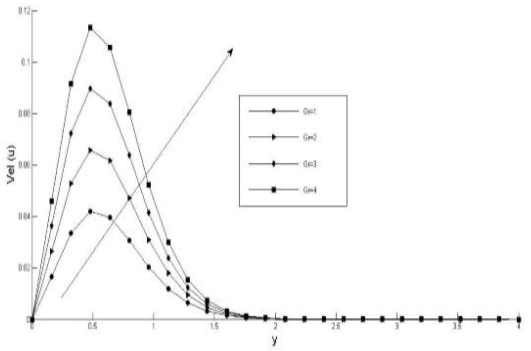

Fig 1: Effect of Gr on Velocity

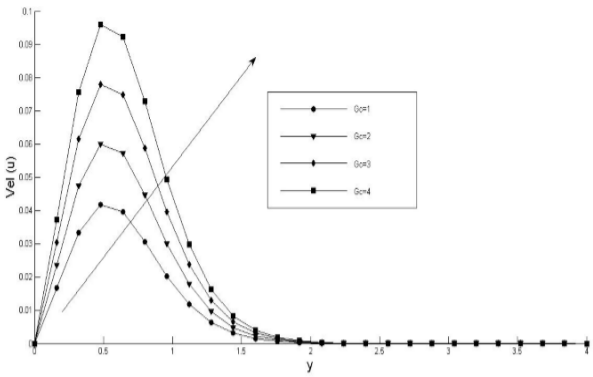

Fig 2: Effect of Gc on Velocity

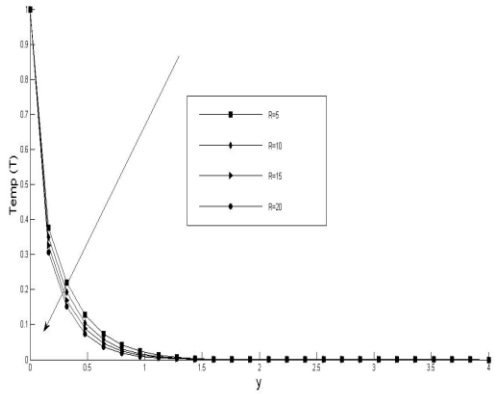

Fig 9: Effect of R on Temperature

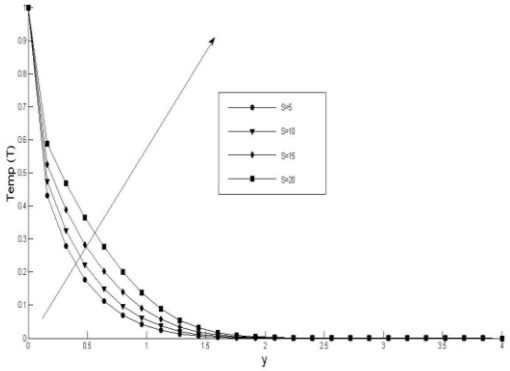

Fig 10: Effect of S on Temperature

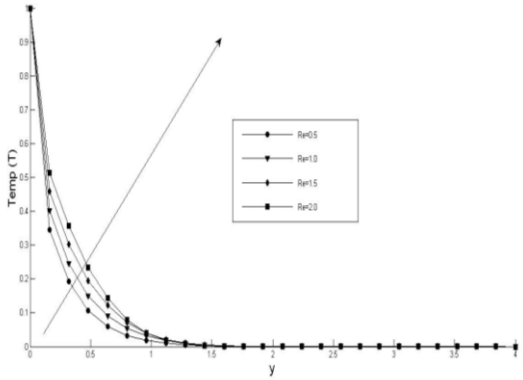

Fig 11: Effect of Re on Temperature

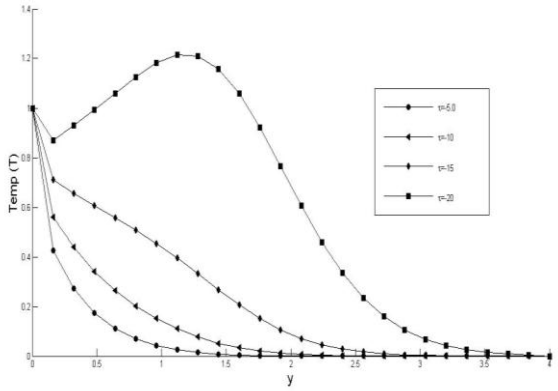

Fig 12: Effect of τ on Temperature

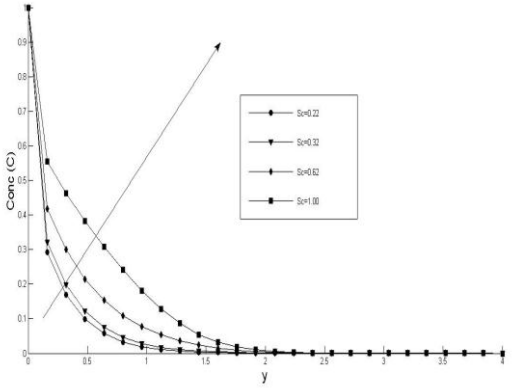

Fig 13: Effect of Sc on Concentration

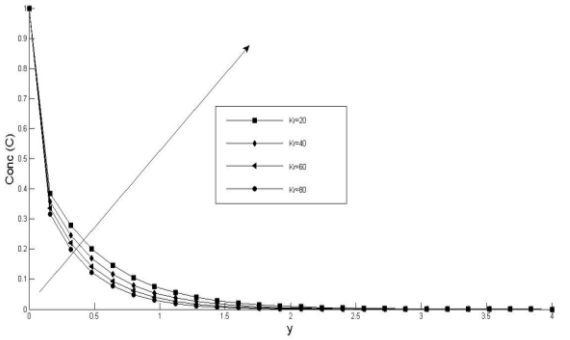

Fig 14: Effect of Kr on Concentration

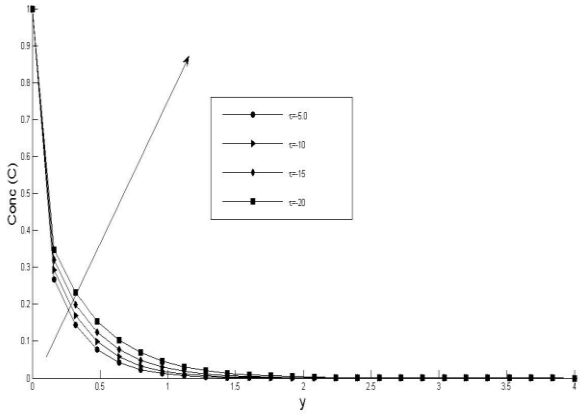

Fig 15: Effect of τ on Concenration

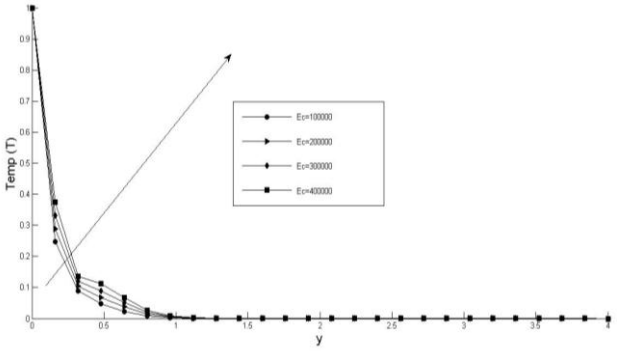

Fig 16: Effect of Ec on Temperature

Tables of Values

In the presence of radiative heat transfer, Reynolds number, and chemical reaction parameter, we formulated and solved approximately the problem of two-dimensional fluid flow. A finite difference method is employed to solve the resulting

coupled partial differential equations. The following are the study's findings:

(1) The skin friction, Nusselt number, and Sherwood number are given in Tables 1 to 3.

(2) The influence of the physical factors Gr, Gc, and M on skin friction is shown in Table 1. When Gr and Gc increase, shear stress increases, but there is no substantial change when M increases.

(3) Table 2 depicts the effect of K, τ , and R physical factors on skin friction and Nusselt number. It has been noted that as K, skin friction increases, while the τ and R decreased as the Nusselt number has increased.

(4) Table 3 shows the effect of physical parameters Ec, Re, and S on the Nusselt number. Heat transmission is shown to increase as Ec, Re, and S rise.

(5) Table 4 shows the influence of various thermophysical parameters on the Nusselt number and Sherwood number. The Nusselt number and Sherwood number both increase as Pr and Sc increase, which explains why the chemical reaction Kr decreases as the Sherwood number increases.

Table 1: shows numerical values for skin friction coefficient C_f , Nusselt number N_u , and Sherwood number S_h for Pr = 0.71, Sc = 0.22, M = 1.0, R = 1, K = 0.1, S = 1, Ec = 0.001.

Gr	Gr	M	C_f	N_u	Sh
1	1	1	0.1037	-5.1129	-6.5352
2	1	1	0.1651	-5.1129	-6.5352
3	1	1	0.2266	-5.1129	-6.5352
4	1	1	0.2881	-5.1129	-6.5352
1	1	1	0.1037	-5.1129	-6.5352
1	2	1	0.1459	-5.1129	-6.5352
1	3	1	0.1881	-5.1129	-6.5352
1	4	1	0.2303	-5.1129	-6.5352
1	1	10	0.1034	-5.1129	-6.5352
1	1	20	0.1030	-5.1129	-6.5352
1	1	30	0.1024	-5.1129	-6.5352
1	1	40	0.1018	-5.1129	-6.5352

Table 2: shows numerical values for skin friction coefficient C_f , Nusselt number N_u , and Sherwood number S_h for Gr = Gc =1.0, Pr = 0.71, Sc = 0.22, M = 1.0, R = 1, K = 0.1, S = 1, for K, τ , R.

K	τ	R	C_f	N_u	Sh
0.01	-4	1	0.0976	-5.1130	-6.5352
0.03	-4	1	0.1027	-5.1130	-6.5352
0.05	-4	1	0.1034	-5.1130	-6.5352
0.07	-4	1	0.1036	-5.1129	-6.5352
0.1	-5	1	0.1032	-4.8884	-6.4885
0.1	-10	1	0.0945	-3.7356	-6.2519
0.1	-15	1	0.0657	-2.5555	-6.0094
0.1	-20	1	0.0148	-1.3982	-5.7606
0.1	-4	5	0.1009	-5.1129	-6.5352
0.1	-4	10	0.0977	-5.6021	-6.5352
0.1	-4	15	0.0948	-5.8273	-6.5352
0.1	-4	20	0.0923	-6.2066	-6.5352

Table 3: shows numerical values for skin friction coefficient C_f , Nusselt number N_u , and Sherwood number S_h for Gr = Gc =1.0, Pr = 0.71, Sc = 0.22, M = 1.0, R = 1, K = 0.1, S = 1, for Ec, Re and S.

Re	Ec	S	C_f	N_u	Sh
0.5	1	1	0.0970	-5.6615	-6.5352
1.0	1	1	0.1037	-5.1129	-6.5352
1.5	1	1	0.1094	-4.5777	-6.5352
2.0	1	1	0.1140	-6.5670	-6.5352
1	1.000	1	0.1000	-4.8884	-6.9477
1	2.000	1	0.1016	-6.0984	-6.9477
1	3.00	1	0.1033	-5.6129	-6.9477
1	4.00	1	0.1050	-5.1105	-6.9477
1	1	5	0.1068	-4.1105	-6.5352
1	1	10	0.1112	-4.4733	-6.5352
1	1	15	0.1220	-4.0249	-6.5352
1	1	20	0.0923	-3.4847	-6.5352

Table 4: shows numerical values for skin friction coefficient C_f , Nusselt number N_u , and Sherwood number S_h for Gr = Gc =1.0, Pr = 0.71, Sc = 0.22, M = 1.0, R = 1, K = 0.1, S = 1, for Kr, Pr and Sc.

Pr	Kr	Sc	C_f	N_u	Sh
0.71	5	0.22	0.0996	-4.2020	-6.5352
1.0	5	0.22	0.1090	-3.3024	-6.5352
3	5	0.22	0.1602	2.9242	-6.5352
7	5	0.22	0.2028	10.0602	-6.5352
0.71	20	0.22	-1.0153	-0.5526	-5.4414
0.71	40	0.22	-1.1016	0.5529	-5.6710
0.71	60	0.22	-0.9952	0.5536	-5.8694
0.71	80	0.22	-0.9862	-3.7356	-6.0432
0.71	5	0.32	0.0945	-3.7356	-6.2519
0.71	5	0.32	0.0975	-3.7356	-5.9707
0.71	5	0.62	0.1064	-3.7356	-5.0997
0.71	5	1.00	0.1179	-3.7356	-3.8869

Conclusion

Fluid flow over a vertical porous plate with variable suction, Reynolds number, and chemical reaction has been examined for heat and mass transfer. The Crank-Nicolson approach was used to solve the problem's dimensional governing equations. Physical parameters such as Reynolds number (Re), Prandtl number (Pr), thermal Grashof number (Gr), species Grashof number (Gm), magnetic field (M), Eckert number (Ec), radiation (R), Schmidtl number (Sc), and chemical reaction parameter (Kr) are graphically and tabulated on flow patterns to highlight their effects. We therefore conclude as follows:

(1) Temperature and velocity increases with increased Reynolds number while magnetic field has a retarding effects on the velocity profile.
(2) A rise in R and M causes reduction in the temperature and velocity profile while a rise in Ec induces a substantial rise in velocity U.
(3) Increase in Pr, Ec, S, and τ causes the temperature profile to reduce, while a rise in τ ,Pr, K, Gr and Gc causes a rise in velocity.
(4) A rise in parameters of Sc, τ and Kr cause the concentration distribution to increase as well.

Conflict of Interest

Authors have declared that there is no conflict of interest reported in this work.

References

Alao F I, Fagbade A I & Falodun B O 2016. Effects of thermal radiation, soret and Dufour effects on an unsteady heat and mass transfer flow of a chemically reacting fluid past a semi-infinite vertical plate with viscous dissipation. *Journal of Nigerian Mathematical Society.*, 35:142-158.

Carnahan B, Luther H A & Wlkes J O 1969. *Applied Numerical Methods.* John Wiley & Sons, New York.

Idowu A S, Dada M S & Jimoh A 2013. Heat and mass transfer of Magnetohydrodynamic(MHD) and dissipative fluid flow pass a moving vertical porous plate with variable suction. *Mathematical Theory and Modeling*. 3(3): 80-102.

Kala B S, Rawat M S, Reddy G V R & Rawat N 2017. Diffussion- thermo and thermo-diffussion effects on MHD fluid flow over Non-Darcy porous medium. *Asia Research Journal of Mathematics.*, 2(2), 1-17.

Modest M S 1993. *Radiation Heat Transfer*. MacGraw-Hill, New York.

Prasad V R, Reddy N B & Muthucumaraswamy 2007 Radiation and mass transfer effects on two-dimensional flow past an impulsively started infinite vertical plate. *International Journal of Thermal Sciences.*, 46(12), 1251-1258.

Raptis & Perdikis (1999) Radiation and free convection flow past a moving plate . *Appl. Mech. Eng.*, 4, 817-821.

Ranson J B & Fluton R E 1985. *Concurrent implementation of the Crank-Nicolson method for heat transfer analysis*, NASA Technical Memorandum 86448, Langley Research Center, Springfield, Virginia, USA.

Rushikumai B & Gangadhar K 2012. MHD free Convectional flow between two parallel porous walls with varying temperature. *International Journal of Engineering.*, 67-72.

Subbakar M K & Gangadhar K 2012. Soret and Dufour effects of MHD free convection heat and mass transfer flow over a streching vertical plate with suction and heat source/sink. *International Journal of Modern Engineering Research*., 2(5), 3458-3468.

Usman H, Uwanta I J & Ahmad S K 2016. Magnetohydrodynamic free convection flow with thermal radiation and chemical reaction effects in the presence of variable suction. *MATEC Web of Conference*.,64: 01002,

Uwanta I J & Usman H 2015. finite difference solutions of Magnetohydrodynamic free convective flow with constant suction and variable thermal conductivity in Darcy-Forehheimer porous medium. *Journal of Mathematics*., 11(1), 42-58.

Uwanta I J & Usman H 2014. Convective heat and mass transfer flow over a vertical plate with nth-order chemical reaction in a porous medium. *International Journal of Scientific Engineering and Technology*., 3(2), 172-185.